JOURNAL OF BACTERIOLOGY, Nov. 1998, p. 5660–5667 Vol. 180, No. 21
0021-9193/98/$04.00+0

Wound-Released Chemical Signals May Elicit Multiple Responses from an *Agrobacterium tumefaciens* Strain Containing an Octopine-Type Ti Plasmid

VIRGINIA S. KALOGERAKI AND STEPHEN C. WINANS*

Section of Microbiology, Cornell University, Ithaca, New York 14853

Received 4 June 1998/Accepted 25 August 1998

The *vir* regions of octopine-type and nopaline-type Ti plasmids direct the transfer of oncogenic T-DNA from *Agrobacterium tumefaciens* to the nuclei of host plant cells. Previous studies indicate that at least two genetic loci at the left ends of these two *vir* regions are sufficiently conserved to form heteroduplexes visible in the electron microscope. To initiate an investigation of these genetic loci, we determined the DNA sequences of these regions of both Ti plasmids and identified both conserved loci. One of these is the 2.5-kb *virH* locus, which was previously identified on the octopine-type Ti plasmid but thought to be absent from the nopaline-type Ti plasmid. The *virH* operon contains two genes that resemble P-450-type monooxygenases. The other locus encodes a 0.5-kb gene designated *virK*. In addition, we identified other potential genes in this region that are not conserved between these two plasmids. To determine (i) whether these genes are members of the *vir* regulon and, (ii) whether they are required for tumorigenesis, we used a genetic technique to disrupt each gene and simultaneously fuse its promoter to *lacZ*. Expression of these genes was also measured by nuclease S1 protection assays. *virK* and two nonconserved genes, designated *virL* and *virM*, were strongly induced by the *vir* gene inducer acetosyringone. Disruptions of *virH*, *virK*, *virL*, or *virM* did not affect tumorigenesis of *Kalanchöe diagramontiana* leaves or carrot disks, suggesting that they may play an entirely different role during pathogenesis.

Agrobacterium tumefaciens has the unique ability to stably modify the genomes of host plants in a way that is beneficial to the bacterium (45). It does this by transferring approximately 15 genes from a 200-kb plasmid (the Ti plasmid) to plant nuclei, where they become covalently integrated into the host genome. This transfer process requires the products of approximately 20 known *vir* genes located on a nontransferred portion of the Ti plasmid (44), as well as a smaller number of chromosomally encoded proteins. Most transferred genes can be categorized into two distinct groups. The first group leads to the production of opines, compounds that are released by the plant and used by the bacterium as nutrient sources (8), while the second group of transferred genes mediates the overproduction of the phytohormones auxin and cytokinin, which interfere with the plant's natural phytohormone balance and cause neoplastic growth, resulting in crown gall tumors (1).

An early event leading to tumorigenesis is the transcriptional induction of the *vir* regulon in response to a variety of chemical signals that are released from plant wounds. The most important of these signals consist of a family of related phenolic compounds, including acetosyringone, that act in combination with extracellular acidity and particular monosaccharides (16). These signals are perceived by the chromosomally encoded sugar-binding protein ChvE and the Ti plasmid-encoded proteins VirA and VirG (2, 18, 40). VirA is a transmembrance sensory histidine kinase which phosphorylates the response regulator VirG (20, 21, 43). Phospho-VirG binds to binding sites designated *vir* boxes found upstream of each *vir* promoter and coordinately activates transcription of these promoters (15, 22).

The previously characterized *vir* regulon includes eight operons (36, 39). Of these, the *virA*, *virB* (6, 23), *virD*, and *virG* operons are essential for tumorigenesis, while *virC* and *virE* are required for efficient tumorigenesis, and *virF* is required for tumorigenesis on certain plant hosts (17). *virH* of the octopine-type Ti plasmid was thought not to be required for tumorigenesis, although none of the available mutations disrupts both genes of the *virH* operon. The *tzs* gene of nopaline-type Ti plasmids, which directs the production of a cytokinin precursor, is also part of the *vir* regulon, but disruptions of this gene have not been described.

In an attempt to identify the homologous regions between octopine-type and nopaline-type Ti plasmids, Engler et al. (11) used the electron microscope to determine which sequences of the octopine-type Ti plasmid pTiAch5 were able to form heteroduplexes with the nopaline-type Ti plasmid pTiC58. This study revealed that these plasmids share four major regions of homology, consisting of approximately 30% of their sequences. At that time, genetic analysis of these regions was extremely rudimentary. In hindsight, we now know that every conserved locus directs a process of fundamental importance to the biology of these plasmids. For example, each conserved gene in one cluster was later shown to encode a *vir* gene (Fig. 1), while most of the nonconserved sequences were later shown to encode insertion sequence (IS) elements. The Engler study identified two conserved genetic loci at the left end of the known *vir* region that were not subsequently studied. The reported positions of these conserved sequences suggested that they might flank the *virH* operon, although our analysis necessitates a reevaluation of these mapping data. Since all the genes in the *vir* region that are essential for tumorigenesis are conserved between the two plasmids, we decided to identify these conserved genes and evaluate their roles in pathogenesis.

MATERIALS AND METHODS

Bacterial strains, plasmids, and media. A348 is a widely used strain that harbors the C58 chromosome and the octopine-type Ti plasmid pTiA6NC, while R10 is a wild-type strain that carries pTiR10, an octopine-type Ti plasmid that is virtually identical to pTiA6NC. All strains and plasmids used in this study are

* Corresponding author. Mailing address: Section of Microbiology, Wong Hall, Cornell University, Ithaca, NY 14853. Phone: (607) 255-2413. Fax: (607) 255-3904. E-mail: scw2@cornell.edu.

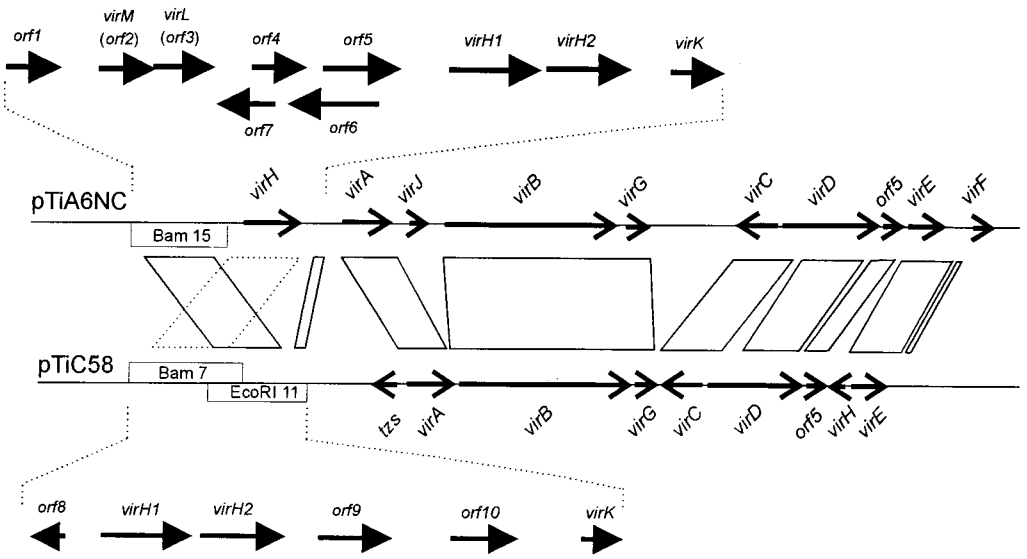

FIG. 1. Octopine- and nopaline-type Ti plasmid *vir* regions. Solid parallelograms represent the regions of homology described by Engler and colleagues (11). The dashed parallelogram indicates the region conserved between these plasmids. Restriction fragments newly sequenced in this study are indicated with white boxes.

described in Table 1. *A. tumefaciens* strains were cultured at 28°C in either LB medium, AB defined medium, or induction broth (3) supplemented, as needed, with 100 μg of kanamycin, carbenicillin, or spectinomycin per ml.

Sequence determination and analysis. Plasmid pCC130 contains *Bam*HI fragment 15 of pTiA6NC, pVIK182 contains *Eco*RI fragment 11 of pTiC58, and pVIK187 contains the partially overlapping *Bam*HI fragment 7 of pTiC58, each introduced into the corresponding sites of pTZ18R. These plasmids were used as templates for double-stranded automated sequencing using *Taq* DNA polymerase, Dyedeoxy Terminator sequencing kits (Applied Biosystems), and an ABI model 373A Stretch DNA sequencer. Sequences were analyzed with the DNASTAR program.

Creation of gene disruptions and *lacZ* fusions. A 7.2-kb *Bam*HI-*Nhe*I DNA fragment containing the *virH* locus was obtained from cosmid pVK219 (27) by digestion with *Bam*HI and *Xba*I and ligated to vector pUC12Cam digested with the same enzymes, creating pVIK193. A 3.0-kb *Eco*47III fragment containing *virH* was deleted and replaced with a 2.1-kb *Sma*I fragment carrying the spectinomycin resistance gene of plasmid pFP45Ω (12), creating plasmid pVIK200. A 5.3-kb *Sal*I fragment of pVIK200 that contains the spectinomycin resistance gene and flanking pTiA6 plasmid DNA was introduced into the suicide vector pWM91 (31), creating pVIK202. pVIK202 was transferred from *Escherichia coli* S17-1/λpir into *A. tumefaciens* R10 by conjugation. Selection for double recombination between pVIK202 and the Ti plasmid was applied by simultaneous selection for resistance to spectinomycin and sucrose, resulting in strain VIK28, which has the *virH* locus replaced by the spectinomycin resistance cassette.

Internal fragments of each of open reading frames (ORFs) *orf1* to *orf7* and *virK* were created by PCR amplification and cloned into suicide vectors pVIK107 or pVIK111 (Table 1), creating an in-frame translational fusion with *lacZ*. The resulting plasmids were conjugally transferred from S17-1/λpir into *A. tumefaciens* A348 and R10 and selected by using kanamycin. To confirm that integration of these suicide plasmids occurred by Campbell-type homologous recombination, we digested the entire genome of these *A. tumefaciens* strains with *Eco*RI, circularized the resulting fragments by using T4 DNA ligase, introduced them into *E. coli* S17-1/λ*pir* by electroporation, and analyzed the rescued plasmids by restriction endonuclease digestion. In each case, the restriction map of the recovered plasmid indicated that a single homologous recombination event had occurred at the predicted site (data not shown).

RNA isolation and RNase S1 protection assays. RNA was purified from strain VIK10 cultured at pH 5.3 in the presence or absence of acetosyringone and from the *virG* mutant strain VIK11 in the presence of acetosyringone (25). RNase S1 protection assays were carried out as previously described (47), using the following oligonucleotides as probes: *orf1*, 5′-CGATTGCGGGGTTAAGATCGT GTCATGCTCGCTTCT-3′; *orf2*, 5′-CCGCGCACCGATTGCCGGAATGATC TGGGTCTCGAATGC-3′; *orf3*, 5′-GGGCGAATGCGAAGCTTCGACGGA GCCTCTCCTGGGTA-3′; *orf4*, 5′-CTATCCGAGGTCATTGTGTCCACAAA CTCCCCAAC-3′; *orf5*, 5′-CGCCATCAATTCTGCAACGGTCGGGGTGCC GGCTCGCAAATA-3′; *orf6*, 5′-CGCGTCCTACATCTGGGCGTATCGCAG CGGTCTTTCG-3′; *orf7*, 5′-GAGCTTGAGGACGCGGATAAGCAGGCTGT TTCCATTCATGGG-3′; *virK*, 5′-CACCGACAAGGATTGTACTGATCCGTT TCATAACTAT-3′; *virG*, 5′-CACGTGAAGGATGTACAATCATCTCCAGA GCCCG-3′; *virB1*, 5′-CCCCGATCTCTTAAACATACCTTATCTCCTTAGCT CGCCCTGG-3′; and *rpoD*, 5′-CCCTTCGCGCGACAGAAGCTCGACGGAA CCCATTTCTATAC-3′. Each oligonucleotide contained four noncomplementary nucleotides at its 3′ end, and removal of these nucleotides ensured that the resistance of the remaining part of the oligonucleotide was due to hybridization. Oligonucleotides complementary to *virB1* and to *rpoD* were used as inducible and constitutive controls, respectively.

Southern hybridizations. Southern hybridization analysis were performed with Zeta-Probe GO blotting membranes according to the procedures described by the manufacturer. Hybridization temperatures used were 65°C for high-stringency and 42°C for lower-stringency conditions. Radiolabeled probes were created by PCR in the presence of [α-^{32}P]dCTP (30).

Cytochrome P-450 difference spectra. The *virH1* gene was cloned as an *Eco*47III-*Ehe*I fragment into the *Sma*I site of pTZ18R, creating pVIK204, while *virH2* was introduced as an *Eco*RV-*Eco*47III fragment into the *Sma*I site of pTZ18R, creating pVIK206. Derivatives of strain JM101 containing pVIK204 or pVIK206 were cultured in 100 ml of LB broth containing carbenicillin (100 μg/ml) to early log phase, treated with isopropyl-β-D-thiogalactopyranoside (IPTG; 1 mM, final concentration), and incubated for an additional 3 h. Cells were collected by centrifugation and disrupted in a French pressure cell. Cellular debris was removed by centrifugation (65,000 × *g* for 30 min). The supernatants were treated with crystalline dithionite and then analyzed across the visible spectrum in the presence and absence of carbon monoxide (28).

Tumorigenesis assays. *A. tumefaciens* wild-type and mutant strains were used for tumorigenesis assays in both *Kalanchoë diagremontiana* leaves (29) and carrot disks (19).

Assays of toxicity of aromatic compounds. Petri dishes containing AB minimal salts, (pH 5.5) and 100 μM acetosyringone, and containing or lacking of 0.04% glucose, were spotted individually with 100 μl of 100 μM solutions of acetosyringone, salisylic acid, 4-hydroxybenzoate, 4-hydroxybenzaldehyde, syringic acid, dimethoxybenzoate, protocatechuate, quinate, ferulate, acetovallone, vanillin, 2,4-dinitrophenol, *trans*-4-hydroxy-3-methoxycinnamic acid, *p*-coumaric acid, 4-hydroxyacetophenone, 3,5-dimethoxyacetophenone, phenanthrenequinone, DL-α,ε-diaminopimelic acid, and 5,5-dithiobis-2-nitrobenzoic acid (all dissolved in dimethylformamide). Three milliliters of top agar (0.5% agar in water) containing approximately 10^7 bacteria that were previously cultured in the presence of acetosyringone and then washed with phosphate buffer (pH 5.5) was poured over these plates and allowed to solidify. Plates were incubated at 28°C for an interval of 5 days and scored for a zone of inhibition.

Nucleotide sequence accession numbers. The sequences reported were deposited in the GenBank DNA sequence database (accession no. AF039888 for sequences from pTiA6NC and accession no. AF034769 for sequences from pTiC58).

RESULTS

Sequence analysis of the left ends of the *vir* regions of pTiA6NC and pTiC58. Figure 1 shows all of the genetic loci in the *vir* region that were identified by Engler and colleagues (11) as being conserved between octopine-type and nopaline-type Ti plasmids (indicated by parallelograms). These conserved sequences include two regions to the left of *virA*, one 2.5

TABLE 1. Strains and plasmids used in this study

Strain or plasmid	Relevant characteristics	Reference
Strains		
A348	C58 chromosome, pTiA6NC (octopine-type) Ti plasmid	37
R10	Wild-type strain with octopine-type Ti plasmid pTiR10	37
KYC55	R10, cured of pTiR10, *arcB*::Tn*5gusA7* Kn^r	5
VIK10	R10 (*virG*::pVIK119) *virG-lacZ virG*$^+$ Kn^r	25
VIK11	R10 (*virG*::pVIK123) *virG-lacZ virG* Kn^r	25
VIK12	R10 (*orf1*::pVIK212) *orf1-lacZ orf1* Kn^r	This work
VIK13	R10 (*virM*::pVIK214) *virM-lacZ virM* Kn^r	This work
VIK14	R10 (*virL*::pVIK127) *virL-lacZ virL* Kn^r	This work
VIK15	R10 (*orf4*::pVIK178) *orf4-lacZ orf4* Kn^r	This work
VIK16	R10 (*orf5*::pVIK150) *orf5-lacZ orf5* Kn^r	This work
VIK17	R10 (*orf6*::pVIK151) *orf6-lacZ orf6* Kn^r	This work
VIK18	R10 (*orf7*::pVIK180) *orf7-lacZ orf7* Kn^r	This work
VIK19	R10 (*virK*::pVIK152) *virK-lacZ virK* Kn^r	This work
VIK20	A348 (*orf1*::pVIK212) *orf1-lacZ orf1* Kn^r	This work
VIK21	A348 (*virM*::pVIK214) *virM-lacZ virM* Kn^r	This work
VIK22	A348 (*virL*::pVIK127) *virL-lacZ virL* Kn^r	This work
VIK23	A348 (*orf4*::pVIK178) *orf4-lacZ orf4* Kn^r	This work
VIK24	A348 (*orf5*::pVIK150) *orf5-lacZ orf5* Kn^r	This work
VIK25	A348 (*orf6*::pVIK151) *orf6-lacZ orf6* Kn^r	This work
VIK26	A348 (*orf7*::pVIK180) *orf7-lacZ orf7* Kn^r	This work
VIK27	A348 (*virK*::pVIK152) *virK-lacZ virK* Kn^r	This work
VIK28	R10 *virH virK* Spec^r	This work
pVIK107	Suicide vector for *lacZ* translational fusions	25
pVIK111	Suicide vector for *lacZ* translational fusions	25
pVIK119	5′ end of *virG* (including promoter) in pVIK111	25
pVIK123	*virG* internal PCR fragment in pVIK111	25
pSW219	Plasmid containing *virA* and a *virB*::*lacZ* fusion	4
pVK219	Cosmid containing *vir* region from pTiA6	27
pWM91	Suicide vector	31
pCC130	*Bam*HI fragment 15 from pTiA6NC cloned into pTZ18R	This work
pVIK127	*virL* internal PCR fragment (codons 83–123) cloned into pVIK107	This work
pVIK150	*orf5* internal PCR fragment (codons 107–256) cloned into pVIK107	This work
pVIK151	*orf6* internal PCR fragment (codons 60–209) cloned into pVIK107	This work
pVIK152	*virK* internal PCR fragment (codons 54–127) cloned into pVIK107	This work
pVIK178	*orf4* internal PCR fragment (codons 20–140) cloned into pVIK107	This work
pVIK180	*orf7* internal PCR fragment (codons 7–129) cloned into pVIK107	This work
pVIK182	*Eco*RI fragment 11 of pTiC58 cloned into pTZ18R	This work
pVIK187	*Bam*HI fragment 7 of pTiC58 cloned into pTZ18R	This work
pVIK193	7.3-kb *Bam*HI-*Nhe*I fragment from pVK219 cloned into pUC12chl	This work
pVIK200	Spec^r cassette from pFP45Ω replacing *virH* locus cloned into pVIK193	This work
pVIK202	5.3-kb *Sal*I fragment from pVIK200 cloned into pWM91	This work
pVIK204	*virH1* cloned into pUC19	This work
pVIK206	*virH2* cloned into pUC19	This work
pVIK212	*orf1* internal PCR fragment (codons 18–83) cloned into pVIK107	This work
pVIK214	*virM* internal PCR fragment (codons 24–103) cloned into pVIK107	This work

and the other 0.5 kb in length, that had not previously been genetically described. According to the Engler analysis, both of these conserved regions are located on *Eco*RI fragment 11 of pTiC58 (Fig. 1). To begin an analysis of the left end of the *vir* region, we sequenced *Bam*HI fragment 15 of pTiA6NC and *Eco*RI fragment 11 of pTiC58. In the latter sequence, we found a 0.5-kb ORF that resembled an ORF that lies between *virH* and *virA* of pTiA6NC. These genes, both designated *virK*, also strongly resemble a gene designated *y4wH* from *Rhizobium* sp. strain NGR234 (Table 2). *virK* evidently represents the conserved region between *virH* and *virA* (Fig. 1). Surprisingly, however, the *Bam*HI fragment 15 of pTiA6NC showed no conservation with *Eco*RI fragment 11 of pTiC58. This made us suspect that there could be an error in the Engler analysis, such that these conserved sequences either do not exist or are located elsewhere.

In an effort to identify the conserved region at the extreme left end of the *vir* region, we completed the sequence of *Bam*HI fragment 7 of pTiC58 (Fig. 1). Unexpectedly, we discovered an operon that strongly resembles the *virH* operon of pTiA6NC (Table 2). This finding was surprising for two reasons. First, *virH* was previously thought to be absent from pTiC58. Second, since these conserved sequences almost certainly represent the remaining conserved sequence identified by the Engler study, it appears that an error had been made in interpreting heteroduplexed DNA fragments (see Discussion).

As might be expected, the newly sequenced regions of both plasmids contained several nonconserved ORFs. Five ORFs (Fig. 1) were identified in *Bam*HI fragment 15, while three were identified in pTiC58 in addition to those described above. We also analyzed two additional ORFs (*orf5* and *orf6*) that were previously (26) sequenced but not characterized (Fig. 1). Of these, the predicted amino acid sequences of *orf5*, *orf8*, and *orf9* resemble genes of various IS elements (Table 2). Interestingly, the first 100 deduced amino acid residues of the *orf10* product are similar to the N-terminus sequence of the VirF proteins of *A. tumefaciens* and *A. vitis* (Fig. 2 and Table 2). No other ORF resembles any known protein sequences, although *orf2* contains a nucleotide-binding motif (GQQGAGKSTL) that matches the highly conserved Walker A consensus sequence (GXXXGK[T/S]) found in many nucleotide-binding proteins (41).

Nuclease S1 protection assays. It was already known that the *virH* operon is strongly induced by the VirA-VirG regulatory system in response to wound-released chemical signals. We

TABLE 2. Amino acid sequence similarities between ORFs found in this study and the products of other sequenced genes

Protein (pTiA6NC)	Homolog	% Identity[a]	% Similarity[b]
VirH1	VirH1 (pTiC58)	73	80
	VirH2 (pTiA6NC)	20	37
	Y4lC (*Rhizobium* sp. strain NGR234)	28	42
	P-450CAM (*Pseudomonas putida*)	24	37
VirH2	VirH2 (pTiC58)	75	80
	VirH1 (pTiA6NC)	29	49
	Y4lD (*Rhizobium* sp. strain NGR234)	25	40
	P-450CAM (*P. putida*)	24	43
VirK	VirK (pTiC58)	72	80
	Y4wH (*Rhizobium* sp. strain NGR234)	64	67
Orf5	IS*1312* (pTiBo542)	73[c]	
	IS*66* (pTiA6)	32	45
Orf8	Y4UI (*Rhizobium* sp. strain NGR234)	49	68
Orf9	Y4QE (*Rhizobium* sp. strain NGR234)	46	64
	Transposase (*Leptospira borgpetersenii*)	38	56
Orf10	VirF (aa[d] 1–100; *Agrobacterium tumefaciens*)	28	54
	VirF (aa 195–310; *A. tumefaciens*)	19	41
	VirF (aa 1–100; *A. vitis*)	30	53

[a] At the amino acid level unless indicated otherwise.
[b] At the amino acid level.
[c] DNA sequence similarity.
[d] aa, amino acids.

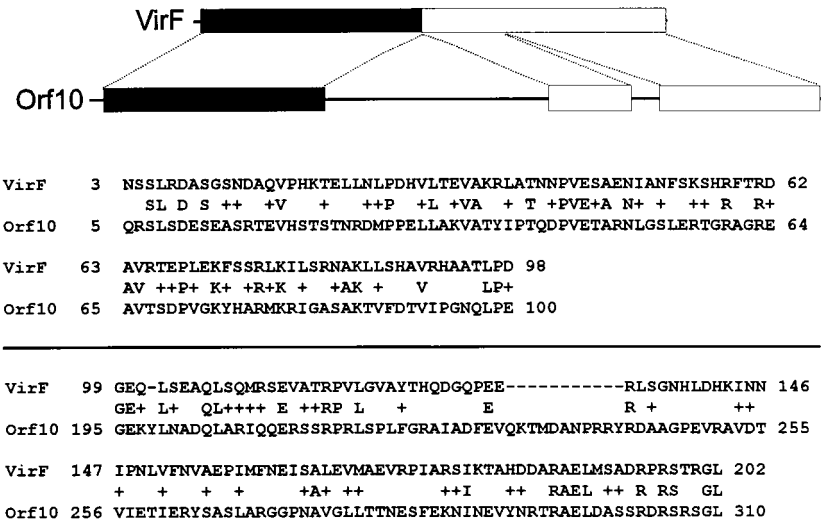

FIG. 2. Sequence similarity between Orf10 of pTiC58 and the VirF of pTiA6. Straight lines represent polypeptide sequence with no similarity. Boxes represent conserved regions; black boxes represent regions of stronger similarity than gray boxes (also see Table 2 for similarity scores).

wanted to determine whether *virK* or any of the nonconserved ORFs found on pTiA6NC was regulated in a similar fashion. To do this, we cultured strain VIK10 (an otherwise wild-type derivative of R10 containing a *virG-lacZ* fusion on the Ti plasmid) in the presence or absence of acetosyringone and cultured strain VIK11 (an isogenic derivative of VIK10 containing a *virG* null mutation [25]) in induction broth containing acetosyringone. We then isolated total RNA from all three cultures and performed S1 protection assays using 5′-radiolabeled oligonucleotides that would hybridize to RNA of each gene. Protection of the probes complementary to *virK*, *orf2*, and *orf3* was strongly enhanced by *vir* gene induction (Fig. 3). In contrast, *orf1*, *orf4*, *orf5*, *orf6*, and *orf7* either are not expressed or are constitutively expressed at low levels.

Translational fusions between Ti plasmid ORFs and *lacZ*. To provide additional evidence for the transcriptional regulation of the ORFs described above, we created gene fusions between them and *lacZ*. This was done by PCR amplifying an internal fragment of each ORF, cloning each fragment into a suicide vector that carries a *lacZ* reporter (25), introducing the vectors into *A. tumefaciens* A348 and R10, and selecting for Campbell-type homologous recombination, which causes integration of the entire plasmid into the corresponding locus. This procedure results in simultaneous disruption of the target gene and fusion of its promoter and translation start site to the *lacZ* reading frame (25).

All strains constructed were assayed for β-galactosidase activity after incubation in the presence and absence of *vir* gene-inducing conditions. The results indicate that *virK-lacZ*, *orf2-lacZ*, and *orf3-lacZ* fusions expressed dramatically elevated β-galactosidase activity in response to *vir*-inducing stimuli, while the remaining five fusions did not respond to these conditions (Table 3). These data are in full agreement with the nuclease S1 protection assays described above (Fig. 3). On the basis of these two kinds of evidence, we conclude that *virK*, *orf2*, and *orf3* are members of the *vir* regulon, while the remaining ORFs are not. We therefore renamed the latter two ORFs *virM* and *virL*, respectively, to indicate that they are coregulated with other *vir* genes. These designations are not meant to imply that these genes are required for tumorigenesis (see below).

Tumorigenesis assays. As described above, each of the eight ORFs described above was disrupted by Campbell-type integration. We tested each strain for the ability to cause neoplastic growth of *K. diagremontiana* leaves or carrot disks. Strains R10 and A348 were used as positive controls. We observed no significant differences between wild-type and mutant strains (data not shown).

One member of the *vir* regulon (*virJ*) encodes a function that is essential for tumorigenesis but functionally redundant with the chromosomal gene *acvB* (24, 35). It seemed plausible that one or more of the three ORFs likewise could encode a function that was essential but genetically redundant. To test this, we carried out Southern hybridizations under conditions of low stringency, probing the genomic DNA of strains A348, A136,

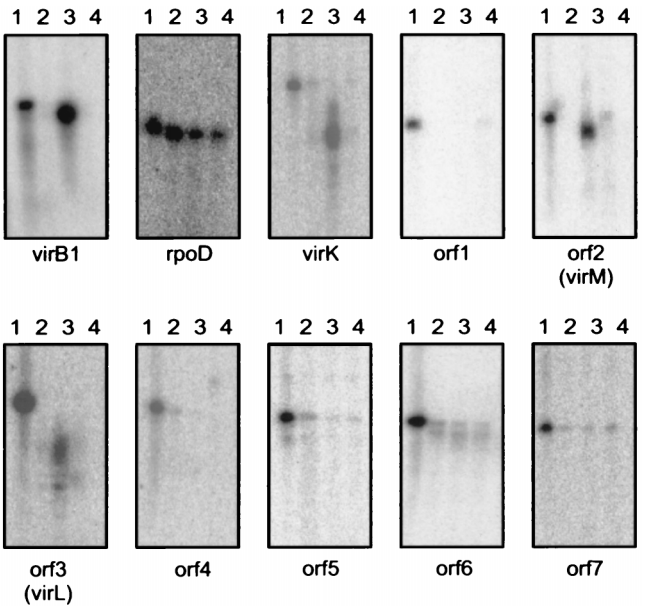

FIG. 3. Nuclease S1 protection assays. Lane 1, oligonucleotide without S1 digestion; lane 2, protection by RNA purified from strain VIK10 cultured without acetosyringone; lane 3, protection by RNA purified from strain VIK10 cultured with acetosyringone; lane 4, protection by RNA purified from strain VIK11 cultured with acetosyringone.

TABLE 3. Induction of *lacZ* fusions by acetosyringone

Strain	*lacZ* fusion in:	β-Galactosidase sp act (Miller units)		
		pH 7.0	pH 5.5	pH 5.5 + acetosyringone
Derivatives of strain R10				
VIK12	*orf1*	0.2	0.3	0.3
VIK13	*orf2* (*virM*)	2	4	119
VIK14	*orf3* (*virL*)	3	3	196
VIK15	*orf4*	0.8	0.8	0.8
VIK16	*orf5*	0.3	0.4	0.5
VIK17	*orf6*	0.3	0.4	0.4
VIK18	*orf7*	0.6	0.5	0.5
VIK19	*virK*	7	13	300
Derivatives of strain A348				
VIK20	*orf1*	0.3	0.2	0.2
VIK21	*orf2* (*virM*)	1	3	61
VIK22	*orf3* (*virL*)	2	3	168
VIK23	*orf4*	0.7	0.7	0.6
VIK24	*orf5*	0.4	0.4	0.3
VIK25	*orf6*	0.2	0.3	0.4
VIK26	*orf7*	0.4	0.4	0.4
VIK27	*virK*	5	9	160

C58, NT1, R10, and KYC55 (a derivative of R10 lacking a Ti plasmid [5]). These DNAs were probed with internal fragments of *virK*, *virL*, and *virM* that were generated by PCR amplification. A probe for the redundant *virJ* gene was included in these experiments, since this gene is known to have a chromosomal homolog (see above). As expected, *virK* sequences were found in strains carrying either a nopaline-type or octopine-type Ti plasmid, but in each case, only a single gene was identified in each strain (Fig. 4). Similarly, only single copies of the *virL* and *virM* genes were found on octopine-type Ti plasmids, and these genes were not detected on the nopaline-type Ti plasmid, indicating that these genes are not conserved between these plasmids. Using a *virJ* probe under identical conditions, we detected both *virJ* and the chromosomal *acvB* gene (data not shown). These data strongly suggest that *virK*, *virL*, and *virM* are each encoded by single genes and that the lack of an effect on tumorigenesis is not due to genetic redundancy.

Construction of an *A. tumefaciens* strain lacking *virH1* and *virH2*. As described above, transposon insertions in the *virH* operon were reported to have either no effect or only subtle effects on tumorigenesis (26, 39). However, sequence analysis of this operon revealed the presence of two related ORFs, designated *virH1* and *virH2*, suggesting that they could be functionally redundant. If so, all previously characterized Tn*3*HoHo1 mutations in this operon would disrupt one but not the other. Furthermore, it was not established which insertions disrupted *virH1* and which disrupted *virH2*. Insertions in *virH1* (if any exist) might not be polar on *virH2*, since not all Tn*3*HoHo1 insertions of exert polar effects (39). To reexamine the possible role of the *virH* operon in tumorigenesis, we created a strain carrying a deletion of the entire operon. Strain VIK28 is a derivative of R10 in which the entire *virH* operon has been replaced with a spectinomycin resistance gene (Fig. 5A; see Materials and Methods). This deletion also removed the first 104 nucleotides of *virK*. Southern hybridization analysis indicated that this deletion has the predicted physical features (Fig. 5B). We observed no significant differences between this mutant and its wild-type parent strain in tumorigenesis of *K. diagramontiana* leaves (data not shown).

Spectral analysis of VirH1 and VirH2. It was previously reported that VirH1 and VirH2 resemble monooxygenases of the P-450 family (26). This family of proteins generally hydroxylate

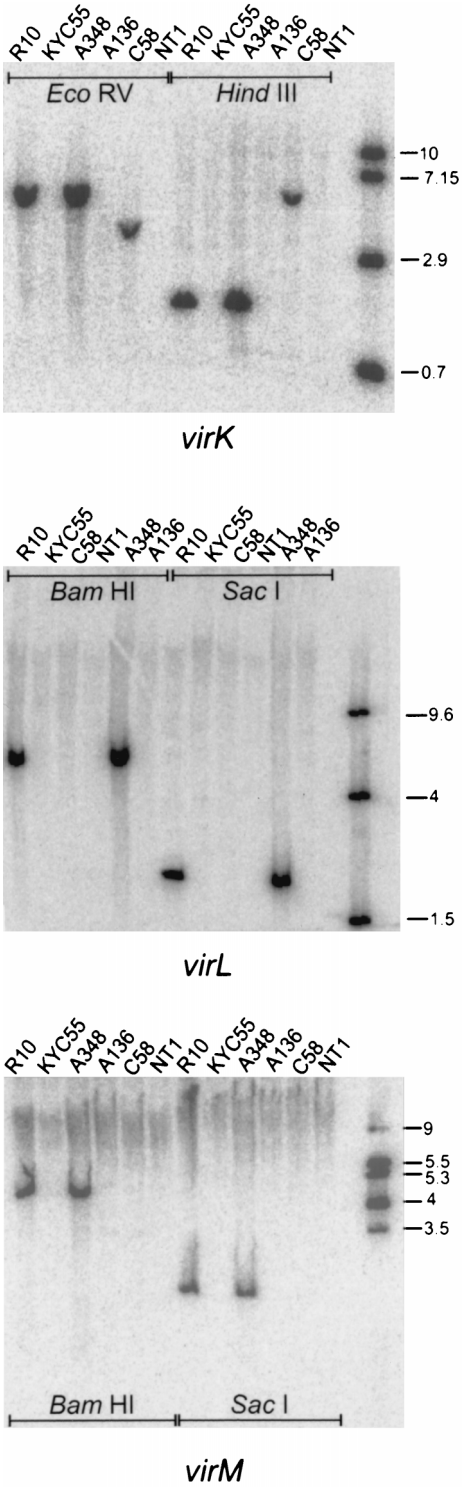

FIG. 4. Low-stringency Southern hybridizations using internal PCR fragments for *virK* (top), *virL* (middle), and *virM* (bottom). The last lane contains molecular mass standards that hybridize to the same probe.

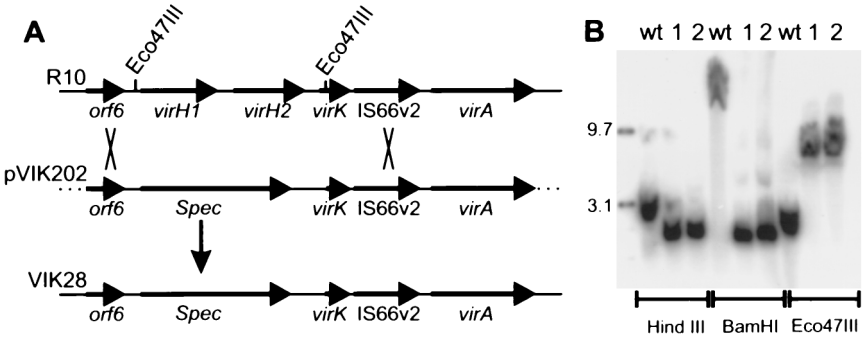

FIG. 5. Replacement of the *virH* locus by a gene mediating resistance to spectinomycin. (A) Double recombination required for this exchange. (B) Southern hybridizations of the parental strain R10 (wt [wild type]) and two identical mutants (1 and 2). The first of these was designated strain VIK28. The extreme left lane contains molecular mass standards that hybridize with the same probe. A PCR fragment lying within *orf6* was used as a probe.

diverse substrates at the expense of molecular oxygen and have varied biological roles in detoxification of toxic compounds, in the catabolism of growth substrates, and in the biosynthesis of secondary metabolites (32). These enzymes show characteristic carbon monoxide difference spectra with a strong peak at 450 nm. Under certain conditions, difference spectra of these enzymes can have a peak at 420 nm rather than 450 nm (34, 42, 46), although such a peak generally indicates that the enzyme is catalytically inactive. To determine the difference spectra of VirH1 and of VirH2, we expressed each protein in *E. coli* (see Materials and Methods). Cleared extracts containing either enzyme showed a carbon monoxide difference spectrum with a prominent peak at 420 nm (Fig. 6). We were not able to find conditions in which a peak at 450 nm was observed.

Since several bacterial P-450 monooxygenases play roles in catabolism of toxic compounds (33, 38), and since plant wound sites are known to contain many compounds that are toxic to microorganisms (9), we wanted to determine whether *virH* or any other member of the *vir* regulon might have a role in detoxification. To do this, we pretreated with acetosyringone three strains, wild-type *A. tumefaciens* strain R10, an isogenic *virH* deletion mutant (VIK28), and an isogenic *virG* mutant (VIK10), and then plated these cultures in top agar on solid medium containing a variety of phenolic compounds (20 compounds in all). Zones of growth inhibition for each compound were identical in size for all three strains, suggesting that no member of the *vir* regulon is involved in the detoxification of these compounds.

DISCUSSION

Our long-term interest in the *vir* regulon of the octopine-type Ti plasmid drew our attention to two DNA fragments that are conserved in the *vir* regions of two widely studied Ti plasmids (Fig. 1) but were previously uncharacterized. These sequences were thought to have been located within *Bam*HI fragment 15 of pTiA6NC and within *Eco*RI fragment 11 of pTiC58. As described above, our sequence analysis indicates that these regions are not conserved and that one of the conserved loci is *virH* itself. The second conserved locus had been previously sequenced in pTiA6NC (26) but not characterized and had not previously been found in pTiC58. At the same time, we also wanted to identify any new members of the *vir* regulon, even if not conserved, since any such genes are by definition induced at the outset of plant infection and are likely to play significant roles in the initial stages of host-microbe interactions.

The *virH* and *virK* loci. Since it was widely believed that *virH* is absent from nopaline-type Ti plasmids, we were quite surprised to identify this operon in *Bam*HI fragment 7 of pTiC58. Since we found no conserved genes in the positions predicted by the Engler study (11), it appears that a mistake had been made in that study in interpretation of the heteroduplexed DNA. While Engler et al. showed a short nonconserved region separating the genes now designated *virH* and *virK* on pTiC58 and a longer one on pTiAch5, we find exactly the opposite and therefore propose that these single-stranded regions separating *virH* and *virK* in the Engler study had been incorrectly assigned.

The *virH* locus consists of two genes that code for proteins of the P-450 family of monooxygenases (32). This locus of pTiA6NC is a member of the *vir* regulon (26) and is therefore induced at the outset of infection. While induction of the pTiC58 *virH* region has not been tested, DNA sequence similarity between these operons extends into the 5′ regulatory region. *virH* was previously believed to be restricted only to octopine-type Ti plasmids and in some cases speculated to account for different properties of these two Ti plasmids (13, 26).

Monooxygenases of the P-450 family acquire their name from their strong increase in absorption at 450 nm when treated with carbon monoxide (34). Several of these enzymes have been shown to have a difference spectrum at 420 nm rather than 450 nm (42, 46). Proteins that absorb at this shorter wavelength (termed P-420 enzymes) are generally catalytically inactive. The P-450CAM protein of *Pseudomonas putida* shows a difference maximum at 450 nm when purified from *P. putida* but under different conditions shows a difference maximum of 420 when expressed in *E. coli* (46). *E. coli* extracts containing VirH1 or VirH2 showed carbon monoxide difference spectra at 420 nm. We were unable to find conditions where extracts containing either protein show a peak at 450 nm. An increase in absorption at 420 nm is nevertheless a hallmark of this family of proteins, and we therefore conclude that VirH1 and

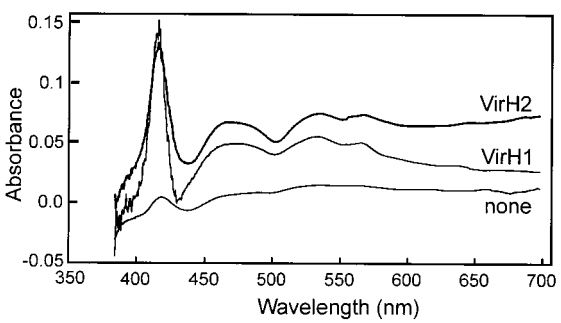

FIG. 6. Carbon monoxide difference spectra of VirH1 and VirH2. Bacterial extracts were prepared as described in Materials and Methods and scanned across the visible spectrum in the presence and absence of carbon monoxide.

VirH2 are probably members of this family and likely to carry out hydroxylation or related oxidation reactions.

Transposon insertions in the *virH* operon have been previously described (26) but not precisely mapped to one or the other of these genes. Since *virH1* and *virH2* are homologous to each other, it seemed plausible that they could be functionally redundant. Because the transposon used to mutagenize this operon (Tn*3*HoHo1 [39]) does not always exert polar effects on downstream genes, even an insertion in *virH1* might not disrupt expression of both genes. We therefore created a deletion of the entire *virH* locus and compared mutant and wild-type strains for the ability to cause tumorigenesis. Our results showed that at least for the plant host tested, *virH* is not required for efficient tumorigenesis.

We also addressed the question of whether these proteins could play a role in detoxifying compounds found at plant wound sites. Members of the family of the P-450 monooxygenases have often been reported to be involved in the detoxification of toxic compounds. For example, P-450CAM of *P. putida* metabolizes the rather toxic compound camphor, in the process converting it to a source of carbon and energy (32). However, neither *virH* nor any member of the *vir* regulon altered the toxicity of any the 20 different phenolic compounds tested.

As described above, the other conserved locus in the Engler study is a gene that we now designate *virK*. This gene was previously sequenced in pTiA6NC but not genetically analyzed (26). We showed that this gene is strongly induced by acetosyringone in a VirG-dependent (and probably VirA-dependent) manner. Disruption of *virK* did not affect tumorigenesis. *virK* strongly resembles a gene designated *y4wH* found on pNGR234a of *Rhizobium* sp. strain NGR234 (14). Directly upstream of *y4wH* is a possible binding site for the NodD transcriptional regulator, suggesting that the product of this gene may play a role at the outset of the nodulation of host legumes. The role of *virK* and its *Rhizobium* homolog in plant-microbe interactions will require additional studies.

Other acetosyringone-inducible loci. We also studied seven previously uncharacterized ORFs that might encode proteins. RNase S1 protection assays (Fig. 3) and translational β-galactosidase fusions (Table 3) revealed that *orf2* and *orf3* are strongly induced by acetosyringone. These ORFs were therefore renamed *virM* and *virL*, respectively, to indicate that the genes are members of the *vir* regulon. Neither protein resembles any other sequenced protein, although VirM has a possible ATP-binding motif (41).

Two different chromosomal backgrounds were used to create single-copy translational fusions between each *orf* and *lacZ*. When the fusions were created in the wild-type octopine strain R10, induction was consistently twofold higher than when strain A348, which harbors a nopaline chromosome and the octopine-type Ti plasmid pTiA6NC, was used. Since pTiA6NC and pTiR10 are virtually identical, these data suggest that the host chromosomal backgrounds played a role in induction. One possibility is that the sugar-binding ChvE proteins are functionally different in these strains. It was previously reported that a particular VirA protein interacts optimally with ChvE from the same chromosomal background (10).

Neither *virM* nor *virL* was required for efficient tumorigenesis of two plants. Southern hybridizations proved that the absence of a tumorigenic phenotype is not due to any homolog found elsewhere on the *A. tumefaciens* genome. We conclude that neither protein plays a critical role in tumorigenesis. They could play more subtle roles in tumorigenesis that are difficult to demonstrate under laboratory conditions. It seems equally plausible that these proteins, as well as VirHI, VirH2, and VirK, carry out roles in pathogenesis that are unrelated to T-DNA transfer. The fact the VirK strongly resembles the product of a *Rhizobium* sp. gene that seems to be under the control of the NodD transcriptional regulator strongly supports this hypothesis. At this point it is difficult even to speculate about what these roles might be. In the case of the *virH*-encoded monooxygenases, a role in phytohormone biosynthesis could be one possibility, since a monooxygenase could convert tryptophan to indoleacetamide (on the pathway to auxin). A monooxygenase could also carry out the hydroxylation step required to convert isopentenyladenine to zeatin, a cytokinin. A P-450 type enzyme has been implicated in cytokinin biosynthesis in *Rhodococcus fasciens* (7).

ACKNOWLEDGMENTS

We thank Jeff Scott for providing preparations of insect microsomal P-450. Many thanks go to J. Shapleigh, C. Fuqua, J. Zhu, S. Jafri, and R. Akakura for helpful suggestions and discussions.

This work was supported by General Medical Sciences award GM42893 from NIH.

REFERENCES

1. **Akiyoshi, D. E., R. O. Morris, R. Hinz, B. S. Mischke, T. Kosuge, D. J. Garfield, M. P. Gordon, and E. W. Nester.** 1983. Cytokinin-auxin balance in crown gall tumors is regulated by specific loci in the T-DNA. Proc. Natl. Acad. Sci. USA **80:**407–411.
2. **Cangelosi, G. A., R. G. Ankenbauer, and E. W. Nester.** 1990. Sugars induce the *Agrobacterium* virulence genes through a periplasmic binding protein and a transmembrane signal membrane. Proc. Natl. Acad. Sci. USA **87:**6708–6712.
3. **Cangelosi, G. A., E. A. Best, G. Martinetti, and E. W. Nester.** 1991. Genetic analysis of *Agrobacterium*. Methods Enzymol. **204:**384–397.
4. **Chen, C.-Y., and S. C. Winans.** 1990. Controlled expression of the transcriptional activator gene *virG* in *Agrobacterium tumefaciens* by using the *Escherichia coli lac* promoter. J. Bacteriol. **173:**1139–1144.
5. **Cho, K., W. C. Fuqua, and S. C. Winans.** 1997. Transcriptional regulation and locations of *Agrobacterium tumefaciens* genes required for complete catabolism of octopine. J. Bacteriol. **179:**1–8.
6. **Christie, P. J.** 1997. *Agrobacterium tumefaciens* T-complex transport apparatus: a paradigm for a new family of multifunctional transporters in eubacteria. J. Bacteriol. **179:**3085–3094.
7. **Crespi, M., D. Vereecke, W. Temmerman, M. V. Montagu, and J. Desomer.** 1994. The *fas* operon of *Rhodococcus fascians* encodes new genes required for efficient fasciation of host plants. J. Bacteriol. **176:**2492–2501.
8. **Dessaux, Y., A. Petit, and J. Tempé.** 1992. Opines in *Agrobacterium* biology, p. 109–136. *In* D. P. S. Verma (ed.), Molecular signals in plant-microbe communications. CRC Press, Ann Arbor, Mich.
9. **Dixon, A.** 1986. The phytoalexin response: elicitation, signalling and control of host gene expression. Biol. Rev. **61:**239–291.
10. **Doty, S. L., M. C. Yu, J. I. Lundin, J. D. Heath, and E. W. Nester.** 1996. Mutational analysis of the input domain of the VirA protein of *Agrobacterium tumefaciens*. J. Bacteriol. **178:**961–970.
11. **Engler, G., A. Depicker, R. Maenhaut, R. Villarroel, M. Van Montagu, and J. Shell.** 1981. Physical mapping of DNA base sequence homologies between an octopine and a nopaline Ti plasmid of *Agrobacterium tumefaciens*. J. Mol. Biol. **152:**183–208.
12. **Fellay, R., J. Frey, and H. Krisch.** 1987. Interposon mutagenesis of soil and water bacteria: a family of DNA fragments designed for in vitro insertional mutagenesis of Gram-negative bacteria. Gene **52:**147–154.
13. **Fortin, C., C. Marquis, E. W. Nester, and P. Dion.** 1993. Dynamic structure of *Agrobacterium tumefaciens* Ti plasmids. J. Bacteriol. **175:**4790–4799.
14. **Freiberg, C., R. Fellay, A. Bairoch, W. J. Broughton, A. Rosenthal, and X. Perret.** 1997. Molecular basis of symbiosis between *Rhizobium* and legumes. Nature **387:**394–401.
15. **Han, D. C., and S. C. Winans.** 1994. A mutation in the receiver domain of the *Agrobacterium tumefaciens* transcriptional regulator VirG increases its affinity for operator DNA. Mol. Microbiol. **12:**23–30.
16. **Heath, J. D., T. C. Charles, and E. W. Nester.** 1995. Ti plasmid and chromosomally encoded two-component systems important in plant cell transformation by *Agrobacterium* species, p. 367–385. *In* J. A. Hoch and T. H. Silhavy (ed.), Two-component signal transduction. ASM Press, Washington, D.C.
17. **Hooykaas, P. J., and A. G. M. Beijersbergen.** 1994. The virulence system of *Agrobacterium tumefaciens*. Annu. Rev. Phytopathol. **32:**157–179.
18. **Huang, M.-L. W., G. A. Cangelosi, W. Halperin, and E. W. Nester.** 1990. A chromosomal *Agrobacterium tumefaciens* gene required for effective plant signal transduction. J. Bacteriol. **172:**1814–1822.
19. **Jen, G. C., and M. D. Chilton.** 1986. Activity of T-DNA borders in plant cell

transformation by mini-T plasmids. J. Bacteriol. **166:**491–499.
20. **Jin, S. G., R. K. Prusti, T. Roitsch, R. G. Ankenbauer, and E. W. Nester.** 1990. Phosphorylation of the VirG protein of *Agrobacterium tumefaciens* by the autophosphorylated VirA protein: essential role in biological activity of VirG. J. Bacteriol. **172:**4945–4950.
21. **Jin, S. G., T. Roitsch, R. G. Ankenbauer, M. P. Gordon, and E. W. Nester.** 1990. The VirA protein of *Agrobacterium tumefaciens* is autophosphorylated and is essential for *vir* gene regulation. J. Bacteriol. **172:**525–530.
22. **Jin, S. G., T. Roitsch, P. J. Christie, and E. W. Nester.** 1990. The regulatory VirG protein specifically binds to a *cis*-acting regulatory sequence involved in transcriptional activation of *Agrobacterium tumefaciens* virulence genes. J. Bacteriol. **172:**531–537.
23. **Kado, C. I.** 1994. Promiscuous DNA transfer system of *Agrobacterium tumefaciens*: role of the *virB* operon in sex pilus assembly and synthesis. Mol. Microbiol. **12:**17–22.
24. **Kalogeraki, V. S., and S. C. Winans.** 1995. The octopine-type Ti plasmid pTiA6 of *Agrobacterium tumefaciens* contains a gene homologous to the chromosomal virulence gene *acvB*. J. Bacteriol. **177:**892–897.
25. **Kalogeraki, V. S., and S. C. Winans.** 1997. Suicide plasmids containing promoterless reporter genes can simultaneously disrupt and create fusions to target genes of diverse bacteria. Gene **188:**69–75.
26. **Kanemoto, R. H., A. T. Powell, D. E. Akiyoshi, D. A. Regier, R. A. Kerstetter, E. W. Nester, M. C. Hawes, and M. P. Gordon.** 1989. Nucleotide sequence and analysis of the plant-inducible locus *pinF* from *Agrobacterium tumefaciens*. J. Bacteriol. **171:**2506–2512.
27. **Knauf, V. C., and E. W. Nester.** 1982. Wide host range cloning vectors: a cosmid clone bank of an *Agrobacterium* Ti plasmid. Plasmid **8:**45–54.
28. **Lee, S. S. T., and J. G. Scott.** 1989. An improved method for preparation, stabilization and storage of house fly (Diptera:Muscidae) microsomes. J. Econ. Entomol. **82:**1559–1563.
29. **Mantis, N. J., and S. C. Winans.** 1993. The chromosomal response regulatory gene *chvI* of *Agrobacterium tumefaciens* complements an *Escherichia coli phoB* mutation and is required for virulence. J. Bacteriol. **175:**6626–6636.
30. **Mertz, L. M., and A. Rashtchian.** 1994. Nucleotide imbalance and polymerase chain reaction: effects on DNA amplification and synthesis of high specific activity radiolabeled DNA probes. Anal. Biochem **221:**160–165.
31. **Metcalf, W. W., W. Jiang, L. L. Daniels, S.-K. Kim, A. Haldimann, and B. L. Wanner.** 1996. Conditionally replicative and conjugative plasmids carrying *lacZ*α for cloning, mutagenesis, and allele replacement in bacteria. Plasmid **35:**1–13.
32. **Munro, A. W., and J. G. Lindsay.** 1996. Bacterial cytochromes P-450. Mol. Microbiol. **20:**1115–1125.
33. **O'Keefe, D. P., J. A. Romesser, and K. J. Leto.** 1988. Identification of constitutive and herbicide inducible cytochrome P-450 in *Streptomyces griseolus*. Arch. Microbiol. **149:**406–412.
34. **Omura, T., and R. Sato.** 1964. The carbon monoxide-binding pigment of liver microsomes. J. Biol. Chem. **239:**2370–2378.
35. **Pan, S. Q., S. Jin, M. I. Boulton, M. Haws, M. P. Gordon, and E. W. Nester.** 1995. An *Agrobacterium* virulence factor encoded by a Ti plasmid gene or a chromosomal gene is required for T-DNA transfer into plants. Mol. Microbiol. **17:**259–269.
36. **Rogowsky, P. M., B. S. Powell, K. Shirasu, T.-S. Lin, P. Morel, E. M. Zyprian, T. R. Steck, and C. I. Kado.** 1990. Molecular characterization of the *vir* regulon of *Agrobacterium tumefaciens*: complete nucleotide sequence and gene organization of the 28.63 Kbp regulon cloned as a single unit. Plasmid **23:**85–106.
37. **Sciaky, D., A. L. Montoya, and M.-D. Chilton.** 1977. Fingerprints of *Agrobacterium* Ti plasmids. Plasmid **1:**238–253.
38. **Shao, Z. Q., and R. Behki.** 1996. Characterization of the expression of the *thcB* gene, coding for a pesticide-degrading cytochrome P-450 in *Rhodococcus* strains. Appl. Environ. Microbiol. **62:**483–487.
39. **Stachel, S. E., and E. W. Nester.** 1986. The genetic and transcriptional organization of the *vir* region of A6 Ti plasmid of *Agrobacterium tumefaciens*. EMBO J. **5:**1445–1454.
40. **Stachel, S. E., and P. C. Zambryski.** 1986. *virA* and *virG* control the plant-induced activation of the T-DNA transfer process of *A. tumefaciens*. Cell **46:** 325–333.
41. **Walker, J. E., M. Saraste, M. J. Runswick, and N. J. Gay.** 1982. Distantly related sequences in the alpha and beta subunits of ATP synthase, myosin, kinases and other ATP-requiring enzymes and a common nucleotide binding fold. EMBO J. **1:**945–951.
42. **Wells, A. V., P. Li, P. M. Champion, S. A. Martinis, and S. G. Sligar.** 1992. Ti resonance Raman investigations of the *Escherichia coli* expressed *Pseudomonas putida* cytochrome P-450 and P-420. Biochemistry **31:**4384–4393.
43. **Winans, S. C., R. A. Kerstetter, J. E. Ward, and E. W. Nester.** 1989. A protein required for transcriptional regulation of *Agrobacterium* virulence genes spans the cytoplasmic membrane. J. Bacteriol. **171:**1616–1622.
44. **Winans, S. C.** 1992. Two-way chemical signaling in *Agrobacterium*-plant interactions. Microbiol. Rev. **56:**12–31.
45. **Zambryski, P.** 1992. Chronicles from the *Agrobacterium*-plant cell DNA transfer story. Annu. Rev. Plant Physiol. Plant Mol. Biol. **43:**465–490.
46. **Yu, C. A., and I. C. Gunsalus.** 1974. Cytochrome P-450cam. II. Interconversion with P-420. J. Biol. Chem. **1:**102–106.
47. **Zhu, J., and S. C. Winans.** 1998. Activity of the quorum-sensing regulator TraR of *Agrobacterium tumefaciens* is inhibited by a truncated dominant defective TraR-like protein. Mol. Microbiol. **27:**289–297.